Through-Resonance Assisted Ionic Hydrogen Bonding in 5-Nitro-*N*-salicylideneethylamine

Tadeusz Marek Krygowski,[†] Krzysztof Woźniak,*[,†] Romana Anulewicz,[†] Dorota Pawlak,[†] Waclaw Kolodziejski,[‡] Eugeniusz Grech,[§] and Anna Szady[§]

Department of Chemistry, University of Warsaw, ul. Pasteura 1, 02-093 Warsaw, Poland, Department of Inorganic and Analytical Chemistry, Warsaw Medical Academy, ul. Banacha 1, 02-097 Warsaw, Poland, and Technical University of Szczecin, ul. Piastów 42, 71-065 Szczecin, Poland

Received: March 4, 1997; In Final Form: September 18, 1997[⊗]

Structural and spectroscopic properties of hydrogen bonding in solid 5-nitro-*N*-salicylideneethylamine have been investigated. This is the first example of ionic [$O^-\cdots H-N^+$] intramolecular hydrogen bonding in a structure of Schiff base. Single-crystal X-ray diffraction and ^{13}C magic-angle spinning NMR show that the title molecule is dominated by ionic canonical structures favored by through molecule conjugation between the nitro group and both groups of salicylidene fragment. Being involved in strong intramolecular [$O^-\cdots H-N^+$] hydrogen bonding, 5-nitro-*N*-salicylideneethylamine forms its crystal lattice by means of different types of weak intermolecular [$O^-\cdots H-N^+$], N−H···O and C−H···O hydrogen bonds. On the basis of the solid-state NMR results, it has been suggested that the acidic proton can also stay at the oxygen atom, and this is qualitatively supported by X-ray diffraction.

Introduction

Imines, >C═N−R, and their derivatives, containing an aryl group bound to nitrogen or carbon, form a significant group of compounds in organic chemistry and are known as Schiff bases.[1] They are products of the condensation of amines with aldehydes and ketones. Schiff bases and their derivatives are subject to ca. 500 publications per year. This includes ca. 200 structural papers. Schiff bases owe such a big popularity to the wide range of their applications in organic synthesis starting from reduction to amines,[2] addition to >C═N bond,[3] radical dimerization,[4] up to applications in synthesis of lactams[5] and addition to the carbonyl atom of ketones.[6]

Schiff bases have been examined by several spectroscopic and diffractometric methods in solution and the solid state. Among others, correlation between ^{13}C NMR chemical shift and the Hammett constants as well as the dual substituent parameters (using σ_I and σ_R[7]) have been reported.[8,9] Also single-proton transfer in naphthol derivatives has been studied using variable temperature ^{13}C NMR in solution and in the solid state.[10−12]

A correlation between structural and spectroscopic parameters of intramolecular N−H···O hydrogen bonding in Schiff bases has been discussed in refs 13−15. Only neutral O−H···N hydrogen bonds are known so far in structures of Schiff bases. Due to the variety of readily accessible structural modifications, Schiff bases are very good model moieties to study intramolecular electronic and structural effects on various chemical and physicochemical properties. In this paper we would like to examine structural and spectroscopic consequences of through-resonance assisted hydrogen bonding in a model compound, 5-nitro-*N*-salicylideneethylamine (NSEA; see Figure 1), which seems to be the first example of a Schiff base containing an ionic intramolecular [$O^-\cdots H-N^+$] hydrogen bond. In particular, we want to discuss possible relationships between the changes of hydrogen bonding and redistribution of electron density of the aromatic fragment.

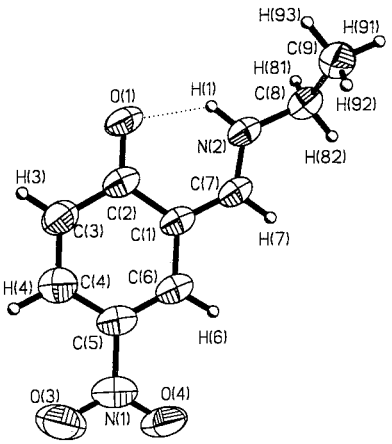

Figure 1. The labeling of atoms in the asymmetric unit and the atomic displacement parameters. An ORTEP drawing of NSEA.

Experimental Section

Solid-state ^{13}C NMR with cross-polarization (CP) and magic-angle spinning (MAS) was done at 50.3 MHz on a Varian UNITY-200 spectrometer using a high-speed double-bearing probehead and silicon nitride rotors spun in dry air. The single-contact ^{13}C CP/MAS experiments were performed at 298 K with the 4 ms contact times for the optimal contact time experiments and 50 μs for the short contact time experiments. The length of the ^1H and ^{13}C $\pi/2$ pulses was 5 μs; the recycle delay, 3 s; and the MAS rate, 5 kHz. The ^{13}C dipolar-dephased spectra[16] (DD) were recorded with a 50 μs delay prior to acquisition. The dipolar-dephased CP experiments expose quaternary carbon lines, and the CP experiments with the short contact time (SCT) highlight lines from carbons with adjacent protons. Ordinary CP/MAS spectra contain all these lines. The ^{13}C NMR spectra of saturated dimethyl sulfoxide (DMSO) and chloroform solutions were recorded at 295 K with a Varian UNITY-500 spectrometer at 125.9 MHz. The assignment was supported by distortionless enhancement by polarization transfer (DEPT) experiments.

X-ray Diffraction. The X-ray measurements were done on a KM-4 KUMA diffractometer with graphite monochromated Cu Kα radiation. The data were collected at room temperature

[†] University of Warsaw.
[‡] Warsaw Medical Academy.
[§] Technical University of Szczecin.
[⊗] Abstract published in *Advance ACS Abstracts,* November 15, 1997.

S1089-5639(97)00814-1 CCC: $14.00

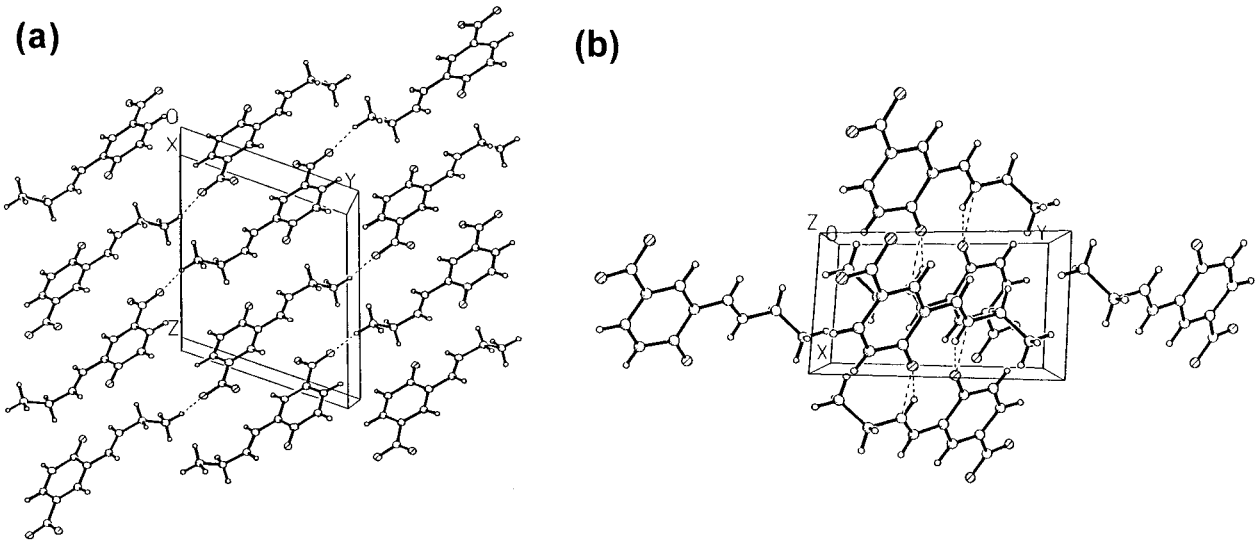

Figure 2. Three-dimensional packing of molecules: (a) view along *X*-axis, (b) view along *Z*-axis.

using ω-2θ scan technique. The intensity of the control reflections varied by less than 3%, and the linear correction factor was applied to account for this effect. The data were also corrected for Lorentz and polarization effects, but no absorption correction was applied. The structure was solved by direct methods[17] and refined using SHELXL.[18] The refinement was based on F^2 for all reflections except those with very negative F^2. Weighted *R* factors, w*R*, and all goodness-of-fit *S* values are based on F^2. Conventional *R* factors are based on *F* with *F* set to 0 for negative F^2. The criterion $F_o^2 > 2\sigma(F_o^2)$ was used only for calculating *R* factors and is not relevant to the choice of reflections for the refinement. *R* factors based on F^2 are about twice as large as those based on *F*. All hydrogen atoms were located from a differential map and refined isotropically. Scattering factors were taken from Tables 6.1.1.4 and 4.2.4.2 in ref 19. Experimental details concerning the collection and refinement of data are listed in Table 1.

TABLE 1: Crystal Data and Structure Refinement Details for NSEA

empirical formula	$C_9H_{10}N_2O_3$
formula weight	194.19
temperature (K)	293(2)
wavelength (Å)	1.541 78
crystal system	triclinic
space group	$P\bar{1}$
unit cell dimensions	$a = 4.988(1)$ Å $\alpha = 68.80(3)°$ $b = 9.102(2)$ Å $\beta = 78.24(3)°$ $c = 11.057(2)$ Å $\gamma = 89.20(3)°$
volume (Å^3)	457.2(2)
Z	2
density (calc) (Mg/m^3)	1.411
absorption coefficient (mm^{-1})	0.907
F(000)	204
crystal size (mm^3)	0.25 × 0.30 × 0.25
θ range for data collection (deg)	4.39−80.74
index ranges	$-6 \le h \le 6$, $-10 \le k \le 11$, $0 \le l \le 13$
reflections collected	2023
independent reflections	1925 [*R*(int) = 0.0684]
refinement method	full-matrix least-squares on F^2
data/restraints/parameters	1918/0/168
goodness-of-fit on F^2	1.093
final *R* indices [$I > 2\sigma(I)$]	*R*1 = 0.0478, w*R*2 = 0.1550
R indices (all data)	*R*1 = 0.0533, w*R*2 = 0.1694
extinction coefficient	0.21(2)
largest diff. peak and hole (eÅ^{-3})	0.20 and −0.17

Results and Discussion

Analysis of X-ray Data. NSEA crystallizes in a general position in the triclinic $P\bar{1}$ space group with two molecules in the unit cell (Table 1). The labeling of atoms in the asymmetric unit and an ORTEP illustration of atomic displacement parameters are given in Figure 1. Positional parameters, the bond lengths and angles, and the numerical values of atomic displacement parameters are collected in the Supporting Information. The packing of the NSEA molecules in the crystal lattice is shown in Figure 2.

The crystal and molecular structure of NSEA reveals a few interesting findings. First, there is a strong intramolecular $N^+-H\cdots O^-$ hydrogen bond in the NSEA molecule with the proton transferred from the oxygen to the nitrogen atom. So far, in all cases studied, the proton in such H-bonds was found at the oxygen atom. Structural parameters of this hydrogen bond, and of some other bonds, are summarized in Table 2. Due to this ionic hydrogen bonding the first part of the chain attached to the aromatic fragment is coplanar with the benzene ring. The same atoms are also involved in a weaker, also ionic, intermolecular hydrogen bond. In this case the acceptor O(1) atom comes from the neighboring symmetry-related molecule of NSEA (X, 1 − Y, 1 − Z). As a result some nice centrosymmetric dimers are formed (Figure 3).

Each NSEA molecule also participates in weak C(7)−H(7)···O(4) and C(6)−H(6)···O(4) hydrogen bonds with the oxygen atom from the nearest nitro group in the crystal lattice (2 − X, 1 − Y, −Z), being—at the same time—an acceptor of such a hydrogen bond via its own O(4) oxygen atom. Due to such interactions, another dimerization takes place (Figure 3). Finally, there is also a short contact between the methyl C(9)−H(92) group and the O(3) (X, Y − 1, 1 + Z) oxygen atom, and this means that also the O(3) oxygen atom from the parent molecule is an acceptor of such a weak hydrogen bond. The details of all of these hydrogen bonds can be found in Table 2, and the final arrangement of molecules bounded via different types of hydrogen bonding is shown in Figure 3.

Additionally, it appears that the phenyl ring in NSEA is strongly deformed from regular hexagon. Usually, the deformations of the ring in 1,2,4-trisubstituted benzene derivatives measured by the aromaticity index HOMA[20] are rather small. The mean value of HOMA for 154 molecular geometries is 0.96,[21] compared to its value for NSEA equal to 0.73. This deformation can be explained by a possible through-resonance effect between the electron-donating OH and the two electron-accepting groups (para NO_2 and ortho C−N═C) in NSEA. When the HOSE model[22,23] is applied to *p*-nitrophenol, the

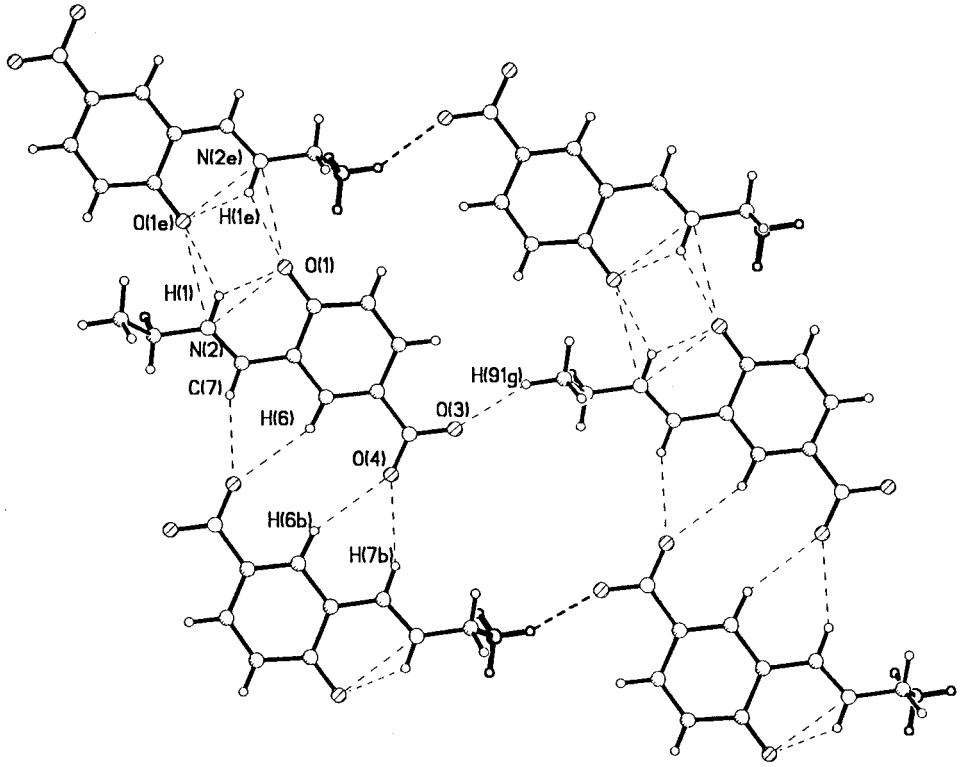

Figure 3. Dimer formation and other weak hydrogen bonds forming a 3D network.

TABLE 2: Structural Parameters of Hydrogen Bonds

hydrogen bond D−H···A sym code	donor−H D−H (Å)	acceptor···H A···H (Å)	donor···acceptor D···A (Å)	D−H···A (deg)
N2−H1···O1	N2−H1	H1···O1	N2···O1	N2−H1···O1
	0.90(2)	1.95(2)	2.646(2)	133(2)
N2−H1···O1	N2−H1	H1···O1	N2···O1	N2−H1···O1
−X, 1 − Y, 1 − Z	0.90(2)	2.24(2)	2.933(2)	134(2)
C6−H6···O4	C6−H6	H6···O4	C6···O4	C6−H6···O4
2 − X, 1 − Y, −Z	0.97(2)	2.54(2)	3.437(2)	153(2)
C7−H7···O4	C7−H7	H7···O4	C7···O4	C7−H7···O4
2 −X, 1 − Y, −Z	0.95(2)	2.44(2)	3.318(2)	155(2)
C9−H92···O3	C9−H92	H92···O3	C9···O3	C9−H92···O3
1 − X, 1 − Y, −Z	0.96(2)	2.79(2)	3.316(2)	156(2)

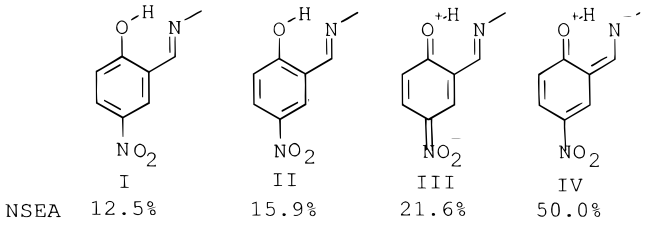

Figure 4. Canonical structures for the aromatic fragment (without proton transfer).

TABLE 3: Aromaticity of NSEA and Some Reference Systems

molecule	HOMA	EN	GEO
α-*p*-nitrophenyl[24]	0.996	−0.003	0.007
β-*p*-nitrophenol[25] [a]	0.994	−0.005	0.011
β-*p*-nitrophenyl[25] [a]	0.984	0.001	0.015
salicylaldoxime[26]	0.960	0.000	0.040
NSEA	0.732	0.030	0.238

[a] There are two independent molecules in the unit cell.

contributions of the quinoid structure are relatively high (17.0−18.7%) for three independent geometries (α plus two *β* forms) of this molecule.[24,25] Similarly, the weight of the quinoid structure for salicylaldoxime is equal to 21.6%.[26] This means that the set of the canonical structures needed to rationalize the intramolecular interactions in NSEA should consist of four of them—including both quinoid structures—as shown in Figure 4. Because of a double through-resonance effect, the oxygen atom in the formal OH group becomes more positive, the OH group more acidic, and in consequence, the acidic proton may be transferred to the N(2) nitrogen atom. This, in turn, leads to a new possibility of an intramolecular charge transfer which increases the weights of canonical structures III and IV. The above be confirmed by the weights of canonical structures estimated by use of the HOSE model[22,23] from the geometry of 5-nitro-*N*-salicylideneethylamine. They are shown in Figure 4.

Undoubtedly, both quinoid structures III and IV contribute considerably to the description of the molecular geometry of NSEA. It seems reasonable to conclude that there is a cooperativity of the ortho and para through-resonance effects and proton transfer from O(1)H group onto the N(2) nitrogen atom. The final consequence of those interactions is the ionic [$O^-\cdots H-N^+$] hydrogen bond and a remarkable deformation of the ring geometry which leads to a considerable decrease of its aromatic character measured by the aromaticity index HOMA.[20] This index is calculated from bond lengths of the π-electron system in question and may be analytically divided into two independent contributions:[27] the energetic one (EN, proportional to the resonance energy) and the geometric one (GEO, accounting for the bond length alternation).

Table 3 shows a comparison of HOMA, EN, and GEO values for NSEA and for *p*-nitrophenol and salicylaldoxime. The far

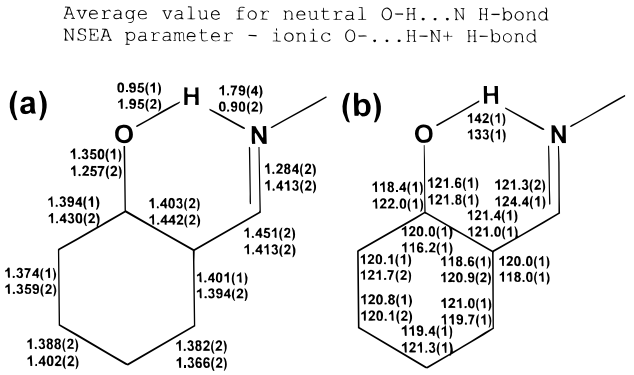

Figure 5. Comparison of data for neutral O−H···N and ionic [O⁻···H−N⁺] H-bonds: (a) bond lengths, (b) valence angles.

greater value of the GEO term for NSEA, as compared to those for salicylaldoxime and *p*-nitrophenol, supports our former conclusion of the cooperative interactions. To study possible differences between the geometries of Schiff bases with [O⁻···H−N⁺] ionic and [O−H···N] neutral H-bonds, we have examined possible molecular fragments similar to a Schiff base with ionic hydrogen bonding and 147 structural fragments containing neutral [O−H···N] H-bonds retrieved from the Cambridge Structural Database.[28] In the case of the ionically H-bonded structures there is only one compound where this kind of bond is observed (REFCODE=LIBPER-[29]). It coexists with neutral O−H···N hydrogen bonding in the other part of the same molecule. There are several structures containing the Schiff base molecular fragment—with a proton transferred from the O to the N atom—being a part of a larger fused aromatic system, which influences the properties of the hydrogen bond of interest. The average geometry of Schiff bases with neutral H-bonding and NSEA is shown in Figure 5. Electron density associated with hydrogen bonding in Schiff bases is conjugated with the electron density in the aromatic part of the molecule. Considering some differences between the geometries of the [O⁻···H−N⁺] and [O−H···N] hydrogen-bonded Schiff bases, one can see that there are profound geometrical differences in the aromatic part of the molecules. Transfer of the proton in Schiff bases from the oxygen atom to the nitrogen one is associated with the shortening of the C_{ar}−O bond which is gaining partly double character due to a decrease in electronegativity of the oxygen atom. This also causes the π-electron density to shift from the aromatic ring toward the oxygen atom and results in a significant elongation of the C(2)C(1) and C(2)C(3) bonds in the aromatic ring. It appears that in the case of the average structure with O−H···N H-bonding the aromatic fragment of Schiff bases is dominated by the Kekule canonical structures—the canonical structures as shown in Figure 4 without the NO_2 group—with contributions of I equal to 27.6% and II 34.2%. In contrast, for the NSEA structure with ionic [O⁻···H−N⁺] H-bonding, the quinoid structures dominates. There are also marked differences in bond lengths and valence angles far from the region of H-bonding, on the opposite site of the molecular fragment. This supports the idea that by proper substitution in the para position (relative to the formal OH group) one can significantly influence the properties of H-bonding in Schiff bases.

Solid-State NMR. The ^{13}C CP/MAS spectra (Figure 6) were assigned as indicated in Table 4. The widest peaks at 163 and 47 ppm are from carbon atoms linked to the nitrogen atom. The latter peak, with the lower chemical shift, must correspond to C(8) in the CH_2 group, so the former is from C(7). The outermost peaks, at 177 and 14 ppm, are assigned on the basis of the chemical shift[30] to C(2) and C(9), respectively. Indeed,

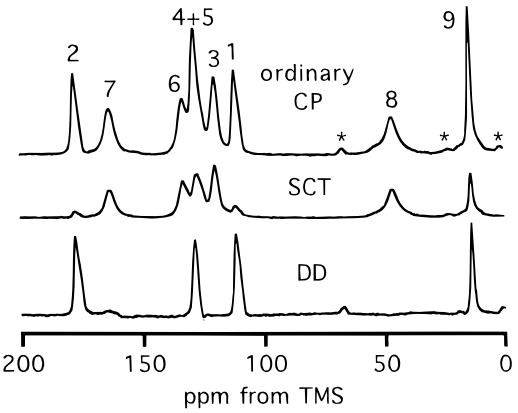

Figure 6. ^{13}C CP/MAS NMR spectra of solid 5-nitro-*N*-salicylideneethylamine.

TABLE 4: NMR Chemical Shifts[a]

	solid state			solution	
carbon	δ (ppm)	SCT	DD	δ in DMSO (ppm)	δ in $CHCl_3$ (ppm)
1	111.7, 109.9[b]	−	+	113.45	115.32
2	177.9, 176.1[b]	−	+	177.92	172.39
3	119.9	+	−	122.80	120.21
4	127.1	+	−	129.18	128.44
5	128.1	−	+	133.41	137.23
6	133.1	+	−	132.62	129.15
7	163.2	+	−	166.50, 166.45[b]	163.88
8	46.7	+	−	46.73	50.37
9	13.6	+	+	14.78	15.33

[a] Plus denotes a prominent peak, and minus denotes a minor or absent peak. The DD experiments expose quaternary carbon lines, and the SCT experiments highlight lines from carbons with adjacent protons. [b] Doublet.

the peak at 177 ppm is from a quaternary carbon atom, because it is present in the DD spectrum and is drastically diminished in the SCT spectrum. The peak at 14 ppm shows up in both the DD and SCT spectra. This is typical of a methyl group, with dipolar interactions reduced by fast group rotation. The remaining peaks in the 100−140 ppm region are from the ring carbons, C(1) and C(3)−C(6). We note that the −HC=N−C_2H_5 group should affect the ring chemical shifts qualitatively similar to the −C≡N group, which decreases the chemical shift of the substituted carbon by 15.4 ppm.[30] In contrast, the NO_2 group increases the chemical shift of the substituted carbon atom by 20.0 ppm.[30] Thus, we assign two quaternary carbon peaks (cf. SCT and DD) at 111 and 128 ppm to C(1) and C(5), respectively. The chemical shift of C(5) is unusually low, and this will be commented on later. There are two peaks left, at 120 and 133 ppm, and three carbon resonances to find [C(3), C(4), and C(6)]. However, consider that the peak at 128 ppm is unusually high and that a peak from a nonquaternary carbon atom appears in this position in the SCT spectrum. It turns out that the peak from C(5) is overlapped with a peak from a proton-bearing carbon atom of the aromatic ring. Indeed, we find slightly different chemical shifts in the SCT and DD spectra of 127.1 and 128.1 ppm, respectively. Considering a mean chemical shift effect in the aromatic ring, calculated from the chemical shift increments from the −OH, −C≡N, and $-NO_2$ groups,[30] the C(3) peak should appear at ca. 112 ppm and the peaks from C(4) and C(6) at ca. 129 ppm. Such calculation cannot provide exact chemical shifts and because there are significant conjugation effects between the groups, we do not know the correct increments for the −HC=N−C_2H_5 group and the −OH group is ionized (cf. the crystallographic structure). Bearing this in mind, we pay attention only to the chemical

TABLE 5: Parameters of the NMR Line Deconvolutions for C(2) and C(1) (See Figure 8)

	C(2)		C(1)	
parameter	1	2	1	2
δ (ppm)	177.91 ± 0.02	176.07 ± 0.07	111.73 ± 0.03	109.87 ± 0.06
FWHM (ppm)[a]	2.04 ± 0.04	2.7 ± 0.1	2.20 ± 0.04	2.48 ± 0.08
peak area (%)	59	41	64	36

[a] FWHM = full width at half-maximum.

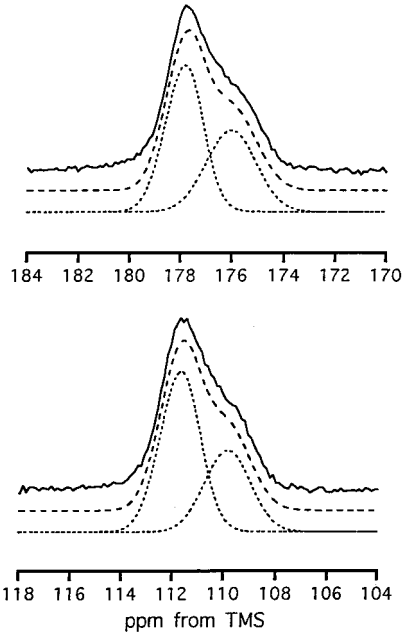

Figure 7. Deconvolutions of the C(2) (top) and C(1) (bottom) DD peaks from solid 5-nitro-*N*-salicylideneethylamine into Gaussian components (see Table 5).

shift order, which indicates that the peak at 120 ppm should be assigned to C(3). The specific assignment of the peaks at 133.1 and 127.1 ppm to C(6) and C(4), respectively, can be done on the basis of the CP efficiency, which increases when the nuclei involved are closer in space.[31] C(6) and C(4) are each linked to one hydrogen atom, but C(4) is relatively close to H(3) (see Figure 1), while C(6) is distant from other protons. Therefore, C(4) is expected to cross-polarize better than C(6), and on the basis of the SCT spectrum it is assigned to the peak at 127.1 ppm.

We are mainly concerned with solid 5-nitro-*N*-salicylideneethylamine, but it is instructive to note that the solid-state chemical shifts are closer to those from the DMSO than from the $CHCl_3$ solution (Table 4). This is because DMSO is involved in the hydrogen bond with the −OH group, so it promotes the ionization of the −OH group. Such ionization, found in the solid state, significantly affects electron density distribution and the ^{13}C chemical shifts because it facilitates intramolecular conjugation with electron-acceptor groups. Consider that the ring −C−O− carbons resonate in the range of ca. 150−165 ppm and that the quinone C═O carbons resonate in the range of ca. 182−190 ppm.[30] Our C(2) has the chemical shift in between those ranges, closer to the latter. This confirms that the CO group in solid 5-nitro-*N*-salicylideneethylamine is significantly involved in the intramolecular conjugation. C(5) is in the para position with respect to the OH group (expected effect of −7.3 ppm[30]) and in the meta position with respect to the $-HC{=}N-C_2H_5$ group (expected effect of +0.6 ppm, by analogy to the −C≡N group[30]). It is amazing that C(5) in the solid sample has the chemical shift characteristic of unsubstituted benzene (128.5 ppm), although we would expect the chemical shift of ca. 140 ppm (128.5 + 20.0 − 7.3 + 0.6). We also stress a large low-frequency shift of several ppm of the C(5) peak from the solid state to the solutions. The $-NO_2$ group in solutions is capable of rotation around the C(5)−N(1) axes, while in the solid state it is forced to be coplanar with the aromatic ring. Again, this facilitates the intramolecular con-

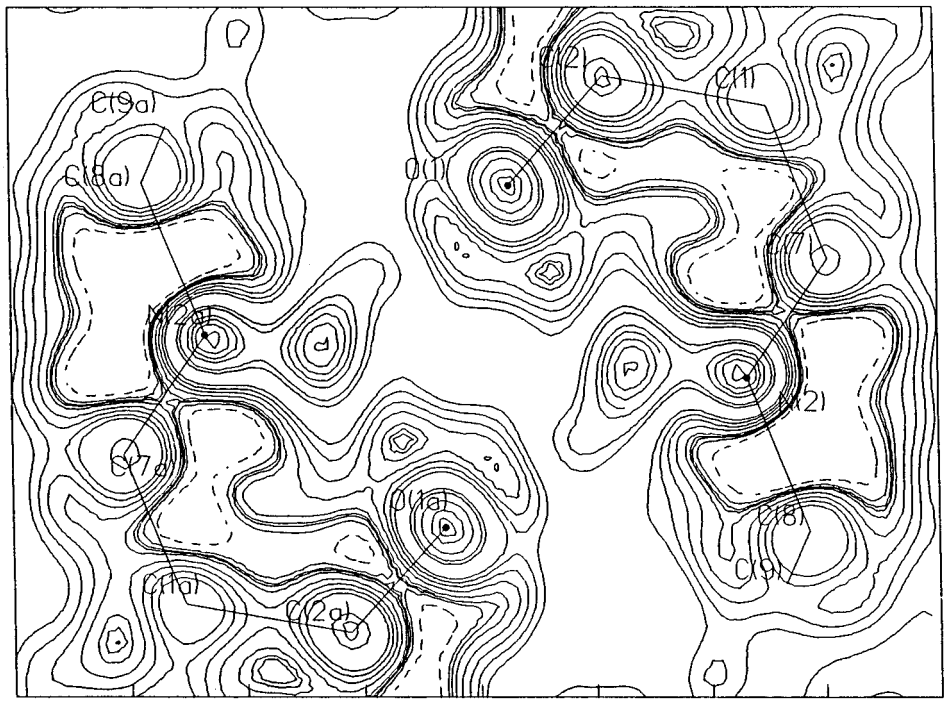

Figure 8. Two-dimensional qualitative electron density map of the H-bonding region. Axes units in angstroms.

jugation of the $-NO_2$ group and markedly affects the C(5) chemical shift.

The most startling effect is the splitting of the C(1) and C(2) peaks from the solid sample (Figure 7, Table 5). The splitting has the same appearance, so it probably has the same reason. The ring carbon peaks C(6) and C(4) are overlapped (the latter also with C(5)) in the ordinary CP spectrum (Figure 6), so we cannot check whether they are split or not. We have carefully examined the C(5) and C(3) peaks, well seen in the NMR spectra (Figure 6). There is no sign of the splitting in the C(5) peak (DD) and in the C(3) peak (ordinary CP). The carbon atoms C(1) and C(2) are substituted and thereby not easily accessible for intermolecular interactions but quite sensitive to electron density redistribution within substituents. Thus, we believe that the splitting is not due to general intermolecular solid-state packing effects,[31] which would possibly affect all the ring carbons. Since the splitting involves the carbon atoms close to the O···H−N intra- and intermolecular hydrogen bonds, we believe that it is related to the hydrogen bonding. A possible explanation would be that the protons in the hydrogen bonds can also be located at the oxygen atoms, and this can be achieved by a concerted proton jump in the hydrogen-bonded dimer.

In fact, we found a tiny peak (ca. 0.2 $eÅ^{-3}$) in the X-ray differential electron density map, located at ca. 0.8 Å from the oxygen atom. However, the refinement of this peak was unsuccessful because the corresponding electron density was too small. On the other hand, the deconvolution of the C(1) and C(2) NMR peaks (Figure 7, Table 5) cannot be directly used for the quantitative assessment of the proton transfer in the hydrogen bond because the CP efficiency is probably dependent on the proton position (different T_{CH} and $T_{1\rho}{}^{H}$ values[32]). We are not aware of any reliable literature reference to the ^{13}C chemical shift effect caused by the proton jump in the hydrogen bond in similar systems. Such effects are likely to be temperature dependent, and the appropriate study is under way. Anyway, despite the different sensitivity of the X-ray diffraction and the NMR spectroscopy in this respect (and their different observation time scales), there is qualitative experimental evidence (Figure 8) from both methods of the coexistence of two forms of the hydrogen bridges.

Conclusions

The first Schiff base containing an ionic intramolecular [O⁻···H−N⁺] H-bond has been described. The structure 5-nitro-*N*-salicylideneethylamine is dominated by ionic canonical structures. There is a double through-resonance effect between the nitro group and both groups of the salicylidene fragment, and this makes the oxygen atom in the intramolecular H-bonding more positive. In consequence, the OH group becomes more acidic and the acidic proton can be transferred to the nitrogen atom. Significant differences in bond lengths and valence angles between Schiff bases with neutral and ionic intramolecular H-bonds, detected also far from the region of H-bonding, indicate that by proper para substitution (relative to the formal OH group) one can significantly influence the properties of the intramolecular H-bonding in the other part of the Schiff base structure. Such conclusions are also supported by the solid-state NMR results.

Being involved in the strong intramolecular [O⁻···H−N⁺] hydrogen bond, 5-nitro-*N*-salicylideneethylamine forms its crystal lattice by means of weak intermolecular [O⁻···H−N⁺], N−H···O, and C−H···O hydrogen bonds.

According to the NMR results, it is probable that the proton occupies two positions within the [O⁻···H−N⁺] hydrogen bond, and this is qualitatively supported by the electron density maps, which show two maxima in the hydrogen bridge.

Acknowledgment. This project was supported by the grant No. 8 S501 039 06 from the Polish State Committee for Scientific Research.

Supporting Information Available: Tables containing atomic coordinates for non-hydrogen atoms and equivalent isotropic displacement parameters for NSEA, bond lengths and angles for NSEA, and anisotropic displacement parameters for NSEA (3 pages). Ordering information is given on any current masthead page.

References and Notes

(1) March, J. *Advanced Organic Chemistry*; Wiley: New York, 1992.
(2) Patai, S. *The Chemistry of Carbon-Nitrogen Double Bond*; Wiley: New York, 1970; p 276.
(3) Harada, K. In *The Chemistry of Carbon−Nitrogen Double Bond*; Patai, S., Ed.; Wiley: New York, 1970; p 266.
(4) Tanaka, H.; Dhimane, H.; Fujita, H.; Ikemoto, Y; Torii, S. *Tetrahedron Lett*. **1988**, *29*, 3811.
(5) Brown, M. J. *Heterocycles* **1989**, *29*, 2225.
(6) Wittig, C.; Frommeld, H. D.; Suchanek, B. *Angew. Chem., Int. Ed. Engl*. **1963**, *2*, 683.
(7) Bromilow, J.; Brownlee, R. T. C.; Lopez, V. O.; Taft, R. W. *J. Org. Chem*. **1979**, *44*, 4766.
(8) Arumugan, N.; Manisankar, P.; Sivasubramanian, S.; Wilson, D. *Org. Magn. Reson*. **1984**, *22*, 592.
(9) Kishore, K.; Sathyanarayana, D. N.; Bhanu, V. A. *Magn. Reson. Chem*. **1987**, *25*, 471.
(10) Vila, A. J.; Lagier, C. M.; Olivieri, A. C. M. *Res. Chem*. **1990,** 28, 29.
(11) Olivieri, A. C.; Wilson, R. B.; Paul, I. C.; Curtin, D. Y. *J. Am. Chem. Soc*. **1989**, *111*, 5525.
(12) Alarcon, S. H.; Olivieri, A. C.; Jonsen, P. *J. Chem. Soc., Perkin Trans. 2* **1993,** 1783.
(13) Bertolasi, V.; Ferretti, V.; Gilli, P.; Issa, Y. M.; Sherif, O. E. *J. Chem. Soc. Perkin Trans. 2*, **1993**, 2223.
(14) Gilli, P.; Bertolasi, V.; Ferretti, V.; Gilli, G.; *J. Am. Chem. Soc*. **1984**, *116*, 909.
(15) Woźniak, K.; He, H.; Klinowski, J.; Jones, W.; Dziembowska, T.; Grech, E. *J. Chem. Soc., Faraday Trans*. **1995**, *91*, 77−85.
(16) Opella, S. J.; Frey, M. H. J. *J. Am. Chem. Soc*. **1979**, *101*, 5854.
(17) Sheldrick, G. M. *Acta Crystallogr*. **1990**, *A46*, 467.
(18) Sheldrick, G. M. *SHELXL93. Program for the Refinement of Crystal Structures*; University of Gotingen, Germany.
(19) *International Tables for Crystallography*, Wilson, A. J. C., Ed.; Kluwer: Dordrecht, 1992; Vol. C.
(20) Krygowski, T. M. *J. Chem. Inf. Comput. Chem*. **1993**, *33*, 70.
(21) Cyrañski, M.; Krygowski, T. M. *J. Chem. Inf. Comput. Sci*. **1996**, *36*, 1142.
(22) Krygowski, T. M.; Anulewicz, R.; Kruszewski, J. *Acta Crystallogr*. **1983**, *B39*, 732.
(23) Krygowski, T. M.; Anulewicz, R.; Wisiorowski, M. *Pol. J. Chem*. **1995**, *69*, 1579.
(24) Coppens, Ph.; Schmidt, G. M. J. *Acta Crystallogr*. **1965**, *18*, 62.
(25) Coppens, Ph.; Schmidt, G. M. J.; *Acta Crystallogr*. **1965**, *18*, 654.
(26) Pfluger, C. E.; Harlow, R. L.; *Acta Crystallogr*. **1973**, *B29*, 2608.
(27) Krygowski, T. M.; Cyrañski, M. *Tetrahedron* **1996**, *52*, 1713.
(28) Allen, F. H.; Davies, J. E.; Galloy, J. J.; Kennard, O.; Macrae, C. F.; Mitchell, E. M.; Mitchell, G. F.; Smith, J. M.; Watson, D. G. *J. Chem. Inf. Comput. Sci*. **1991**, *31*, 187.
(29) Edwards, A. J.; Hoskins, B. F.; Robson, R.; Wilson, J. C.; Moubaraki, B.; Murray, K. S. *J. Chem. Soc., Dalton Trans*. **1994**, 1837.
(30) Wehrli, F. W.; Wirthlin, T. *Interpretation of Carbon-13 NMR Spectra*; Heyden & Son Ltd.: London, 1978.
(31) Fyfe, C. A. *Solid State NMR for Chemists*; CFC Press: Ontario, 1983.
(32) Mehring, M. *High Resolution NMR Spectroscopy in Solids*; Springer-Verlag: Berlin, 1976; Chapter 4.